



Preparation of amine group-containing chelating fiber for thorough removal of mercury ions

Nianfang Ma^a, Ying Yang^a, Shuixia Chen^{a,b,*}, Qikun Zhang^a

^a PCFM Lab, OFCM Institute, School of Chemistry and Chemical Engineering, Sun Yat-Sen University, 135 Xingang Road West, Guangzhou 510275, PR China

^b Materials Science Institute, Sun Yat-Sen University, Guangzhou 510275, PR China

ARTICLE INFO

Article history:

Received 5 January 2009

Received in revised form 27 April 2009

Accepted 1 June 2009

Available online 7 June 2009

Keywords:

Chelating fiber

Amine group

Mercury

Adsorption

Low residual concentration

ABSTRACT

An aminated chelating fiber (AF) with high adsorption capacity for mercury ions was prepared by grafting copolymerization of acrylonitrile onto polypropylene fiber, followed by aminating with chelating molecule diethylenetriamine. Effects of reaction conditions such as temperature, reaction time, bath ratio and dosage of catalyst on the grafting yield were studied. Chemical structure, tensile strength and thermal stability of AF were characterized. The adsorption performances for mercury were evaluated by batch adsorption experiments and kinetic experiments. The results show that AF is effective for the removal of mercury over a wide range of pH. The chelating fiber also shows much higher adsorption capacities for mercury, the equilibrium adsorption amount could be as high as 657.9 mg/g for mercury. The high adsorption capacity of Hg²⁺ on AF is resulted from the strong chelating interaction between amine groups and mercury ions. Two amine groups coordinate with one mercury ion could be speculated from the adsorption capacity and amine group content on AF. The kinetic adsorption results indicate that the adsorption rates of AF for mercury are very rapid. Furthermore, the residual concentration was less than 1 µg/L with feed concentration of mercury below 1 mg/L, which can meet the criterion of drinking water, which indicates that the chelating fiber prepared in this study could be applied to low-level Hg contaminated drinking water purification.

© 2009 Elsevier B.V. All rights reserved.

1. Introduction

Mercury is well known for its extremely high toxicity and the serious threat to human life and natural environment [1]. The drinking water criterion for mercury established by USEPA is 2 µg/L [2], and the permitted discharge limit of wastewater for total mercury is 10 µg/L [3]. So it is very important to reduce the residual mercury concentration below the safety limit for mercury ions from industrial wastewater, especially from drinking water.

So far, numerous methods were used to remove mercury, including chemical precipitation, coagulation, reverse osmosis, ion exchange [4], chelating [5,6] and adsorption [7]. However, these methods are not efficient enough to remove very low concentration of mercury ions [8]. Therefore, in order to meet the demand of residual concentration lower than 2 µg/L in drinking water purification, it is necessary to explore adsorptive materials with high adsorption speed and good removal performance for low concentration

mercury ions. As well known, chelating adsorbents are effective to remove mercury ions [9]. Many chelating resins have been reported, but show limited applicability because of their poor hydrophilicity, small surface area, low adsorption rate and poor adsorption capacity in low-concentration mercury solutions [10,11]. Meanwhile, chelating fiber is a very promising adsorption material which possesses high adsorption rate and large adsorption capacity due to its low mass transfer resistance and large external surface area. It can make up these advantages to some extent by choosing suitable chelating group that possesses strong affinity toward mercury. However, in the recovery of mercury, chelating fiber was seldom investigated.

The adsorption efficiency for heavy metal ions by chelating fiber is usually affected by the surface functional groups of the adsorbents [12–14]. The amino group has been found to be one of the most effective chelating functional groups for the adsorption or removal of heavy metal ions from aqueous solution [15]. Of interest are amino functional groups because of their strong affinity toward mercury [6,7]. In the present investigation, an aminated chelating fiber (AF) with high adsorption capacity for mercury ions was prepared by amination of acrylonitrile grafted on the polypropylene fiber, the structure, stability and adsorption behaviors for mercury of this chelating fiber were studied.

* Corresponding author at: School of Chemistry and Chemical Engineering, Sun Yat-Sen University, Guangzhou 510275, PR China. Tel.: +86 20 84112093; fax: +86 20 84034027.

E-mail address: cscsx@mail.sysu.edu.cn (S. Chen).

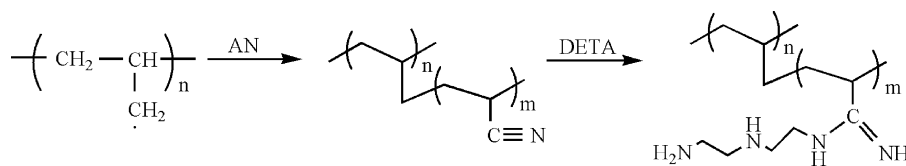


Fig. 1. Synthesis chart of AF.

2. Experimental

2.1. Materials and reagents

All reagents were of analytical grade, and all solutions were prepared with super-pure water (water treated by ion exchange and then purified by reverse osmosis). Glasswares used were repeatedly washed with HNO₃ and rinsed with super-pure water, according to a published procedure [16]. Polypropylene (PP) fiber was manufactured by Zhongshan Xinshun Special Fiber Co., Ltd. The filament had a diameter of 80 μm. Diethylenetriamine (DETA) and mercury(II) chloride (HgCl₂·2H₂O) were purchased from Sigma–Aldrich Co. Nitric acid (HNO₃), acrylonitrile (AN), Mohr's salt (NH₄FeSO₄), dimethylformamide (DMF), hydrochloric acid (HCl), aluminum chloride (AlCl₃·6H₂O) were used as received. Commercial resin 717 (Shanghai Resin Factory, 65–160 mesh).

The reference and working solutions were diluted daily from stock mercury solution (2000 mg/L). Tin (II) chloride (SnCl₂) (10%, w/v) used as reducing agent was prepared by dissolving SnCl₂·2H₂O in 0.5 M H₂SO₄. The pH was adjusted with the following buffer solutions: HNO₃ for pH 1.0; H₂C₂O₄/NaHC₂O₄ for pH 2.0 and 3.0; CH₃COONa/CH₃COOH for pH 4.0–6.0; Na₂HPO₄/NaH₂PO₄ for pH 7.0; Na₂B₄O₇/NaOH for pH 8.0–11; NaOH for pH 12–14.

2.2. Preparation of chelating fiber

2.2.1. AN grafted on PP fiber

The radiation process and amination reaction with DETA of the grafted AN are shown in Fig. 1. PP fibers cleaned with acetone were sealed in a polyethylene bag and subjected to γ-rays irradiation in the presence and absence of air for a certain time. The dose rate of radiation was 0.837 kGy/h. After irradiation, the pre-irradiated PP (PP-ir) fibers with enough dryer were sealed and placed in a refrigerator at 4 °C.

A certain amount of catalyst, AN and PP-ir fiber with different ratios were added into a 200 ml three-neck flask, then bubbled with nitrogen during reaction to remove oxygen. The grafting reaction was carried out at fixed temperature for a certain time. After reaction, the grafted fibers were extracted in a Soxhlet apparatus with DMF to remove the residual monomer and homopolymer. The obtained PP grafted AN (PP-AN) fibers were dried in a vacuum oven at 50 °C for 48 h and then weighed. The degree of grafting (G%) is obtained according to the following formula:

$$G\% = \frac{W_g - W_o}{W_o} \times 100 \quad (1)$$

where W_o and W_g are the weight of the original and grafted fiber, respectively.

The amount of AN grafted on PP fiber was also calculated based on the content of nitrogen in the grafted fiber which was determined by an elemental analyzer.

2.2.2. Amination reaction of PP-AN

The procedures of amination reaction of PP-AN are as follows: the PP-AN fibers, 100 ml of DETA and 4.0 g of AlCl₃·6H₂O were added into a 250 ml flask and suspended by a stirrer. The excess DETA was used as both the solvent and reactant. The reaction was

carried out at 120 °C for 3 h. Then the aminated fiber (AF) was washed with super-pure water and ethyl alcohol, and dried at 50 °C under vacuum.

2.3. Structure measurements and mechanical test

The electron spin resonance (ESR) spectra of pre-irradiated PP fibers were recorded on a JES-FEIXG (JEOL, Ltd.) spectrometer, equipped with a dedicated data station for storage and manipulation of the spectra, an NMR gauss meter for the calibration of the magnetic field and a frequency counter for the determination of the factors. Seed samples of the PP-ir fiber were packed in quartz sample tubes and put in the cavity of the ESR instrument. Spectra were recorded with the following settings: operating frequency 9.44 GHz (X-band), microwave power 4 mw, receiver gain 1×10^3 , scan width ± 250 G, center magnetic field 3360 G, and sweep time 0.1 s.

Infrared spectra were obtained with FT-IR Analyzer (Nicolet/Nexus 670). FT-IR-ATR measurements were carried out at a range of 4000–650 cm⁻¹, equipped with a continuum microscope and ATR objective. Elemental Analyzer (Vario EL) was used for elemental analysis.

Thermogravimetry (TG) Analyzer (NetzschTG-20) was used for thermal stability characterizations of all samples. The thermograms were obtained under a nitrogen atmosphere at a uniform heating rate of 10 °C min⁻¹ from ambient temperature to 600 °C.

The mechanical properties of the fibers were characterized by tensile strength and elongation rate. All tensile testing was performed with an analog controller and equipped with a 100 kN load cell. Breaking load was measured in terms of the breaking force in CentiNewton (cN). Ten stochastic filaments of each sample were tested with 10 mm of the gauge length and 10 mm min⁻¹ of the stretching speed. Then the mean value was calculated.

2.4. Batch procedure

The samples (0.1 g of each) were added into 100 ml of the mercury solutions in the 200 ml Erlenmeyer flasks and adjusted to desired pH. Then the flasks were sealed and shaken for 24 h at 30 °C. The effect of pH value on the non-competitive adsorption was studied at pH 1.0–14.0, by using 100 mg/L of the mercury solution. The pH value of the solutions was adjusted with buffer solutions.

Considering mercury precipitation in higher concentration, the equilibrium adsorption experiments were conducted at pH 7.0 in batch modes. The effect of the initial concentration of the metal ions on the non-competitive adsorption capacity was investigated in the range of 20–2000 mg/L as well as the adsorption time was investigated in the range of 0–24 h. Buffer solution is used to control the pH. The adsorption amount was calculated as follows:

$$Q = \frac{V(C_0 - C_e)}{w} \quad (2)$$

where Q is the adsorption amount (mg/g), w the weight of the AF (g), V the volume of solution (L), and C_0 and C_e are the concentrations (mg/L) of mercury ions before and after adsorption, respectively.

Table 1

The orthogonal experimental table of the effect of various reaction conditions on grafting yield.

Sample no.	T (°C)	t (h)	Bath ratio (ml/g)	Catalyst dosage (wt%)	Grafting yield (%)
1	50	1	20	0	3.2
2	50	3	30	0.1	2.9
3	50	5	40	1	3.1
4	60	1	30	1	7.5
5	60	3	40	0	33.9
6	60	5	20	0.1	45.2
7	70	1	40	0.1	169
8	70	3	20	1	216
9	70	5	30	0	282
I	9.2	179.7	264.4	319.1	
II	86.6	252.8	292.4	217.1	
III	667	330.3	206	226.6	
I/3	3.1	59.9	88.1	106.4	
II/3	28.9	84.3	97.5	72.4	
III/3	222.3	110.1	68.7	75.5	
Range	219.3	50.2	28.8	34	

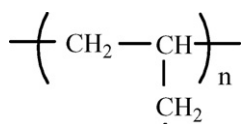
2.5. Adsorption kinetics

Kinetic experiments at different initial concentrations were performed in a batch mode. Initial concentrations of mercury solutions were set at 0.1, 0.5, 1, 10 and 100 mg/L at pH 12. Samples of the flask solution were taken out at certain intervals for analyses of the mercury concentrations.

3. Results and discussion

3.1. Effects of reaction conditions on grafting yield of PP-AN

Three peaks appeared in the ESR spectra of the PP-ir fiber and indicated the type of radicals on the fiber as follows, according to Laura Andreozzi et al. [17,18]:



Factors that affect the grafting yield such as temperature (T), reaction time (t), bath ratio and catalyst dosage are taken into consideration. According to the trial test, three levels are chosen for each factor, so the L_9 (3^4) orthogonal experimental table was chosen to prepare PP-AN, the experimental conditions and the results are listed in Table 1. From Table 1, it is clear that the temperature and reaction time are the main factors that affect the grafting yield. Among all samples prepared, sample 9 get the highest grafting yield and its experimental conditions were chosen for further reaction.

3.2. Structure of the chelating fiber

Fig. 2 shows the IR spectra of PP-ir, PP-AN, AF and AF chelated with mercury. The peaks for the PP-ir fiber can be assigned as follows: 2924 cm^{-1} and 2842 cm^{-1} ($\gamma_{\text{C-H}}$ asymmetric and symmetric in CH, CH_2 groups), 1380 cm^{-1} ($\delta_s\text{CH}_2$), 1450 cm^{-1} ($\delta_s\text{CH}$), where γ represents a stretching vibration and δ_s represents a scissor vibration. Comparing with the spectrum of the PP-ir fiber, a new absorption peak of 2250 cm^{-1} ($\text{C}\equiv\text{N}$ stretching) was observed in PP-AN, which confirm that AN has been grafted onto PP fiber. After the amination reaction of the PP-AN fiber with DETA, the spectrum of the AF changes obviously. The broad absorption band in the range of $3200\text{--}3400\text{ cm}^{-1}$ is much stronger and wider, which is probably due to the superposition of the absorption of the stretching vibrations of N-H in -NH and -NH₂ groups of DETA, the new

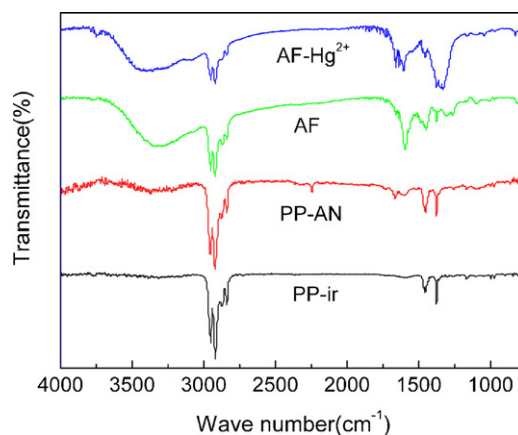


Fig. 2. FT-IR spectra of PP-ir, PP-AN, AF and AF chelated mercury ions.

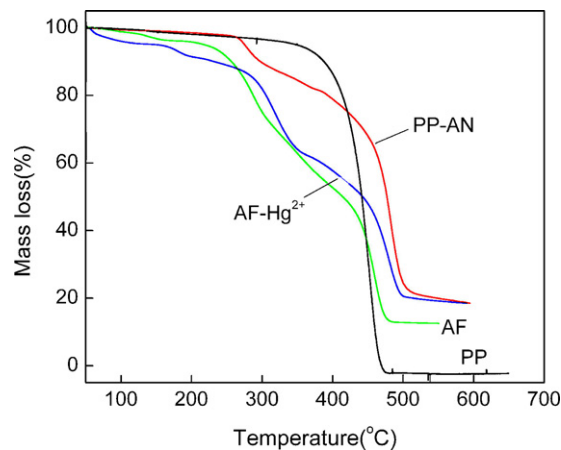


Fig. 3. TGA thermograms of the PP-ir fiber, PP-AN, AF fiber and AF fiber with mercury ions loaded.

peak at 1601 cm^{-1} could be assigned to the stretching of amine groups, which was not observed in the PP-AN fiber. Besides, the absorption peak of 2250 cm^{-1} disappeared. These results indicate that $\text{C}\equiv\text{N}$ of AN has been aminated and DETA was grafted onto the fiber [19,20]. From the FT-IR spectra of the AF-Hg²⁺ complex, it can be seen that the peak for NH₂ at 1601 cm^{-1} became weaker, absorption band at 3310 cm^{-1} get broader and a little red-shift; and a new peak arose at 1730 cm^{-1} for AF-Hg²⁺. All these changes are probably caused by forming complex between AF and mercury, more electrons delocalized extensively among vacant d orbit of mercury and p orbit of NH₂.

3.3. Thermal and mechanical properties of the chelating fibers

The TGA results of PP-ir fiber, PP-AN, AF fiber, and AF fiber loaded with mercury are presented in Fig. 3. The PP-ir fiber was converted into CO₂ and H₂O completely at a certain temperature, which behaves as a 100% mass loss in the experiment. Besides, there is only one platform in the decomposition process of PP-ir fiber. In the case of PP-AN and AF, there are two platforms and the starting decomposition temperature are $270\text{ }^\circ\text{C}$ and $210\text{ }^\circ\text{C}$, respectively. It is believed that the first platform comes from the easy degradation nature of the grafted molecules, such as AN and DETA. And the lower decomposition temperature may be due to the reduced crystallinity of PP that resulting from grafting and amination [20]. It has been reported that the thermal stability of modified fiber depends on their crystallinity [21]. With respect to the AF with mercury ions loaded, after the initial loss of moisture and desorption of gases at

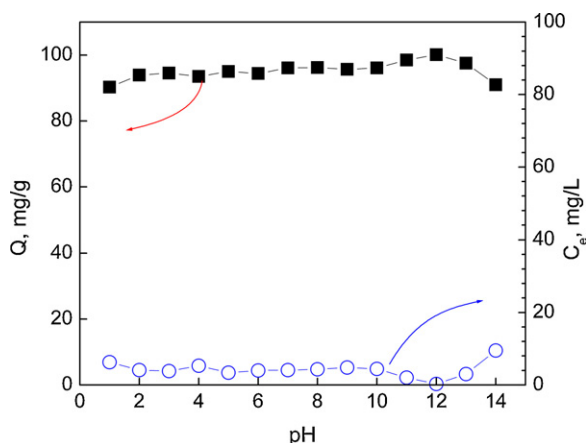


Fig. 4. Effect of pH on the adsorption capacity of AF for mercury [$C_0 = 100 \text{ mg/L}$; $t = 24 \text{ h}$; $T = 30^\circ \text{C}$].

about $100\text{--}200^\circ \text{C}$, there are also two platforms in TG curve. However, char yield of AF fiber with mercury ions loaded is higher than that of PP-ir fiber and the fresh AF, which is due to that mercury adsorbed by AF cannot be decomposed. This result is different with that reported by Coskun et al. [14]. They observed that the char yield of chelating fiber with metal ions loaded is less than that of chelating fiber. The elongation and tensile strength of PP, AF are 2.3 mm and 7.67 cN/tex, 2.0 mm and 5.88 cN/tex, respectively. The results show that there are both a decrease in the elongation and tensile strength of AF fiber. The reason is obviously attributed to the damage of fibers by irradiation.

3.4. Batch adsorption

3.4.1. Effect of pH on adsorption

The type of the species of mercury in solutions depends strongly on the pH of solution. According to stability constant calculations, it was found that $\text{Hg}(\text{OH})_2$ is dominant at $\text{pH} > 4.0$; and while $\text{pH} < 4.0$, HgCl_2 was the main species in the presence of Cl^- [22]. Considering the forms of the ions at different pH value, the effect of pH is studied from pH 1.0 to 14.0, and the results are shown in Fig. 4. Surprisingly, it can be seen that the adsorption amount of AF for mercury is almost not affected by pH value. It is different from the results by Liu et al. [16], which indicates that the sorption quantity of mercury increases with the increasing pH values. They thought that protons could compete with mercury ions, occupying the active adsorbent sites of mercury imprinted copolymers below pH 3.0. Our results in this study are consistent with the observations of Gupta et al. [23] and Balarama Krishna et al. [24].

It is of concern if the mercury precipitates at a higher pH range when $\text{Hg}(\text{OH})_2$ is dominated, Zhang et al. had done the solubility of mercury vs. solution pH in the absence of the adsorbent, and found that no significant change of dissolved mercury at pH range of 1–12 with a initial concentration lower than 120 mg/L [25], which implies that $\text{Hg}(\text{OH})_2$ still dissolves in the solution when mercury concentration is not too high. It is evident that AF is effective for the removal of mercury over a wide range of pH, and the most suitable value is 12, so the further adsorption experiments were carried out at pH 12 if not specified.

3.4.2. Adsorption isotherms

The equilibrium adsorption amount of AF for mercury was investigated over a range of mercury initial concentrations. The results are shown in Fig. 5. It can be seen clearly that the adsorption amount of mercury ions increases with the increasing initial concentrations and reaches a plateau at higher concentration, which resulted from

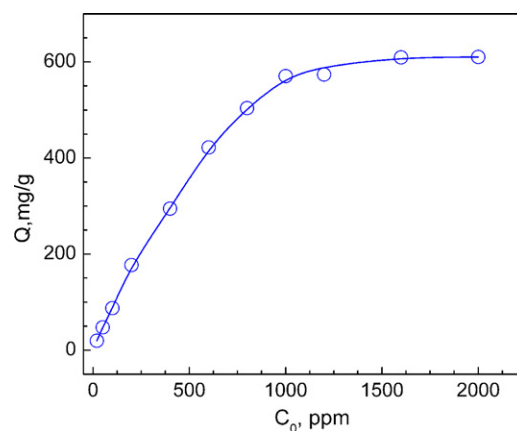


Fig. 5. Effect of initial concentration on the adsorption capacity of AF for mercury [$\text{pH} 7$; $t = 24 \text{ h}$; $T = 30^\circ \text{C}$].

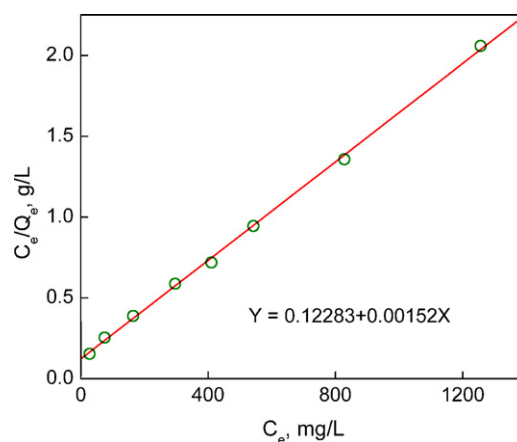


Fig. 6. Linear fitting using Langmuir equation for the adsorption of mercury on AF.

the saturation adsorption of mercury on the chelating sites of the AF.

Equilibrium data were fitted with the Langmuir adsorption equation which is given as

$$Q_e = \frac{Q_m C_e}{1/b + C_e} \quad (3)$$

where Q_e is the amount of mercury adsorbed onto the AF at equilibrium, Q_m is the maximum amount of adsorption (mg/g), b is the adsorption equilibrium experimental constant (1/mg), C_e is the mercury concentration (mg/L) in the solution at equilibrium, and Q_e and b are related to adsorption capacity and energy of adsorption, respectively. The plot of C_e/Q_e vs. C_e for mercury is shown in Fig. 6. The relationship between C_e/Q_e and C_e shows a linear curve, which indicates the adsorption behavior of AF obey Langmuir isotherm model. From the Langmuir equation, the maximum adsorption capacity of the AF was calculated to be 657.9 mg/g for mercury. According to the result of element analysis, the content of N is 12.0%. And two amine groups could coordinate with one mercury ion. So we can calculate that the maximum adsorption capacity is 857.1 mg/g. It may be speculated that the chelating mechanism is mainly chelating interaction between nitrogen-containing functional groups and mercury ions. Besides, it is a monolayer adsorption.

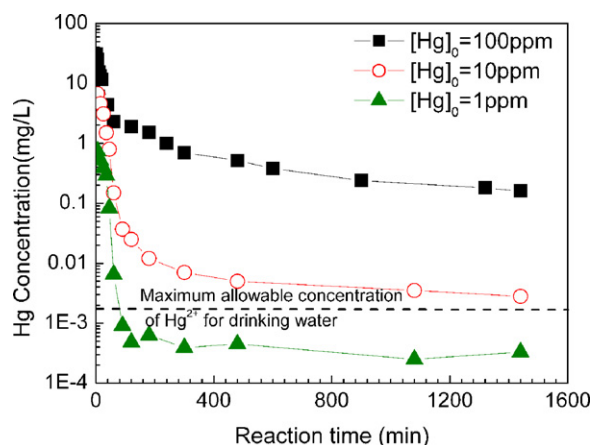


Fig. 7. Adsorption kinetics of AF for mercury ions with various concentrations [pH 12; $C_0 = 100 \text{ mg/L}$; $T = 30^\circ \text{C}$].

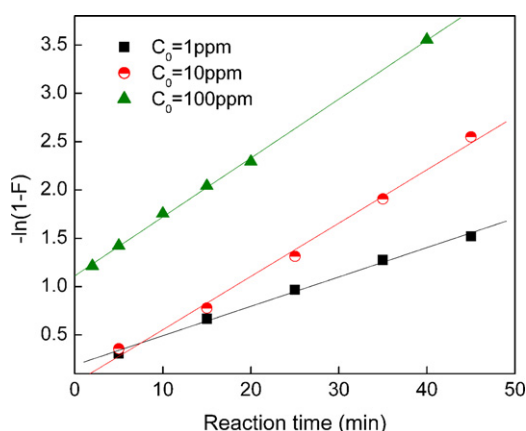


Fig. 8. Plots of $-\ln(1-F)$ vs. t .

3.5. Adsorption kinetics

The dynamic adsorption results of the chelating fiber for mercury are presented in Fig. 7, which shows the tendency of adsorption amounts for mercury on the AF vs. adsorption time. It can be seen that mercury removed by the AF increased sharply with the increasing of adsorption time and achieved adsorption equilibrium after 2 h. Besides, the equilibrium time is independent on the initial mercury concentration. The experimental results in Fig. 7 can be converted into the linear plots of $-\ln(1-F)$ vs. t (Fig. 8) according to the kinetic adsorption equation:

$$-\ln(1-F) = kt + c \quad (4)$$

where t is the adsorption time, k is the adsorption rate constant and c is a constant, F is the ratio of the adsorption amount at time t (Q_t) to that at equilibrium (Q_e). The adsorption rate constants of the ions calculated from the slopes of the plots are 0.03 min^{-1} , 0.055 min^{-1} and 0.061 min^{-1} for the initial mercury concentration of 1 mg/L, 10 mg/L, 100 mg/L, respectively. The results indicate that the adsorption rates of AF for mercury are rapidly, it can be proved from the results in Fig. 7. It can be also concluded that the adsorption rate is higher with a higher mercury concentration, which can be explained by that high mercury concentration accelerates the diffusion of mercury from the bulk solution onto the AF, owing to the increase in the driving force of the concentration gradient [26].

To investigate the application of AF in drinking water purification, adsorption for the ppb level of mercury was examined and the results are shown in Fig. 9. Similar results with that of ppm level of

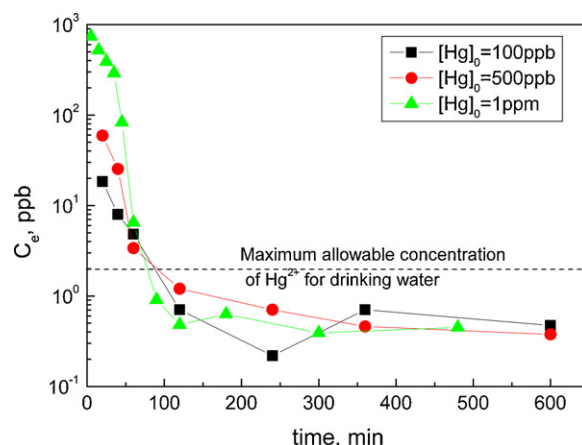


Fig. 9. Adsorption kinetics of AF for mercury ions of low concentrations [pH 12; $T = 30^\circ \text{C}$].

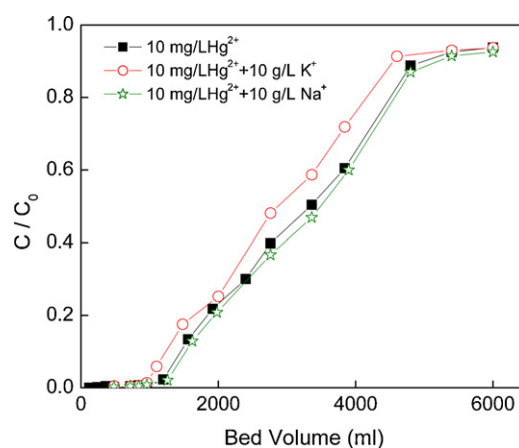


Fig. 10. Breakthrough curves of mercury adsorption on AF while high concentration of K or Na ions coexist [$C_0 = 10 \text{ ppm}$; pH 12; $T = 30^\circ \text{C}$].

mercury were obtained. Mercury ions in solution can be completely removed by AF even its concentration is very low. The residual concentration of mercury in solution could be lower than 2 ppb, which indicates that AF is not only fit for wastewater treatment, but also for drinking water purification.

3.6. Interference of other ions

The interference of other ions on adsorption of AF for mercury were investigated by adding 1000-times excess of Na^+ , K^+ to 10 mg/L Hg^{2+} , respectively. The results in Fig. 10 show that the presence of 1000-times of Na^+ or K^+ in the solution almost do not reduce the adsorption ability of the AF for mercury. The breakthrough curves of mercury adsorption on AF with the coexistence of 1000-times of Na^+ or K^+ ions were almost the same as that without the presence of Na^+ or K^+ ions.

3.7. Breakthrough curves for low-level mercury

In view of applying AF in drinking water purification, the inlet concentration of mercury was 1 mg/L, a commercial amine resin 717 was used as reference to compare the adsorption performance with that of AF. Fig. 11 shows the breakthrough curves of mercury for AF and Resin 717. It can be observed that effluent concentration of mercury start to rise up after 1.8 L of permeation volume for resin, and the tendency is more obvious that the effluent concentration gradually increases with the increased permeation volume,

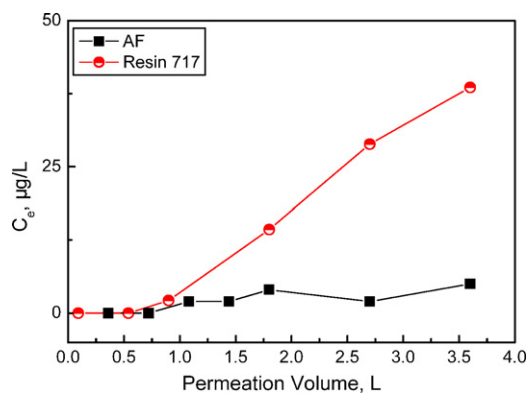


Fig. 11. Breakthrough curves of low concentration of mercury adsorption on AF and resin [$C_0 = 1$ ppm; pH 12; $T = 30^\circ\text{C}$].

whereas that of AF remained nearly 0, which indicates that AF is a very promising adsorbent for mercury removal in drinking water purification.

4. Conclusion

A chelating fiber containing amine and amide groups that could effectively remove mercury ions was successfully prepared by grafting copolymerization of the acrylonitrile onto polypropylene fiber, and then followed by aminating with chelating molecule DETA. It is found that the aminated fiber keep good mechanical strength and thermal stability. With optimal grafting conditions, the grafting degree could be as high as 280%. The chelating fiber shows much higher adsorption capacities for mercury owing to the higher affinity of the amine groups for mercury. The equilibrium adsorption amount could be as high as 657.9 mg/g for mercury and the residual concentration can achieve less than 1 $\mu\text{g/L}$ for feed concentration of mercury lower than 1 mg/L. The results indicate the great application potential of the chelating fiber in drinking water purification.

Acknowledgements

The authors gratefully acknowledge the financial support provided by the Key Program of Science and Technology of Guangdong province (project no. 7117638), Science and Technology Project of Guangdong province (2008B010600039) and Ph.D. Programs Foundation of Ministry of Education of China (200805580007).

References

[1] K.H. Nam, S. Gomez-Salazar, L.L. Tavlarides, Mercury(II) adsorption from wastewaters using a thiol functional adsorbent, *Ind. Eng. Chem. Res.* 42 (2003) 1955–1964.
 [2] USEPA, National Primary Drinking Water Standards, Report EPA 816-F-01-007, EPA, Washington, DC, 2001.

[3] J.A. Ritter, J.P. Bibler, Removal of mercury from waste water: large-scale performance of an ion-exchange process, *Water Sci. Technol.* 25 (1992) 165–172.
 [4] S. Chiarle, M. Ratto, M. Rovatti, Mercury removal from water by ion exchange resins adsorption, *Water Res.* 34 (2000) 2971–2978.
 [5] A.A. Atia, A.M. Donia, K.Z. Elwakeel, Selective separation of mercury (II) using a synthetic resin containing amine and mercaptan as chelating groups, *React. Funct. Polym.* 65 (2005) 267–275.
 [6] J. Chwastowska, E. Kosiarska, Synthesis and analytical characterization of a chelating resin loaded with dithizone, *Talanta* 35 (1988) 439–442.
 [7] J.U.K. Oubagaranadin, N. Sathyamurthy, Z.V.P. Murthy, Evaluation of Fuller's earth for the adsorption of mercury from aqueous solutions: a comparative study with activated carbon, *J. Hazard. Mater.* 142 (2007) 165–174.
 [8] J. Choong, K.H. Park, Adsorption and desorption characteristics of mercury(II) ions using aminated chitosan bead, *Water Res.* 39 (2005) 3938–3944.
 [9] A.A. Atia, A.M. Donia, A.M. Yousif, Synthesis of amine and thiol chelating resins and study of their interaction with zinc(II), cadmium(II) and mercury(II) ions in their aqueous solutions, *React. Funct. Polym.* 56 (2003) 75–82.
 [10] Y. Baba, K. Ohe, Y. Kawasaki, S.D. Kolev, Adsorption of mercury(II) from hydrochloric acid solutions on glycidylmethacrylate-divinylbenzene microspheres containing amino groups, *React. Funct. Polym.* 66 (2006) 1158–1164.
 [11] G. Zuo, M. Muhammed, Selective binding of mercury to thiourea-based coordinating resins, *React. Funct. Polym.* 27 (1995) 187–198.
 [12] M. Chanda, G.L. Rempel, A superfast sorbent based on textile-grade poly(acrylonitrile) fiber/fabric. Rapid removal of uranium from mildly acidic aqueous solutions of low concentration, *Ind. Eng. Chem. Res.* 42 (2003) 5647–5655.
 [13] D.H. Shin, Y.G. Ko, U.S. Choi, W.N. Kim, Synthesis and characteristics of novel chelate fiber containing amine and amidine groups, *Polym. Adv. Technol.* 15 (2004) 459–466.
 [14] R. Coskun, C. Soykan, M. Sacak, Adsorption of copper(II), nickel(II) and cobalt(II) ions from aqueous solution by methacrylic acid/acrylamide monomer mixture grafted poly(ethylene terephthalate) fiber, *Sep. Purif. Technol.* 49 (2006) 107–114.
 [15] H. Yoshitake, T. Yokoi, T. Tatsumi, Adsorption of chromate and arsenate by amino-functionalized MCM-41 and SBA-1, *Chem. Mater.* 14 (2002) 4603–4610.
 [16] Y. Liu, X. Chang, D. Yang, Y. Guo, S. Meng, Highly selective determination of inorganic mercury(II) after preconcentration with Hg(II)-imprinted diazoaminobenzene-vinylpyridine copolymers, *Anal. Chim. Acta* 538 (2005) 85–91.
 [17] L. Andreatto, V. Castelvetro, G. Ciardelli, L. Corsi, M. Faetti, E. Fatarella, F. Zulli, Free radical generation upon plasma treatment of cotton fibers and their initiation efficiency in surface-graft polymerization, *J. Colloid Interface Sci.* 289 (2005) 455–465.
 [18] E. Szajdzinska-Pietek, K. Sulak, I. Dragutan, S. Schlick, ESR study of aqueous micellar solutions of perfluoropolyether surfactants with the use of fluorinated spin probes, *J. Colloid Interface Sci.* 312 (2007) 405–412.
 [19] Y.G. Ko, D.H. Shin, U.S. Choi, Cu crystal growth on a chelating fiber with different amine chain lengths, *Macromol. Rapid Commun.* 25 (2004) 1324–1329.
 [20] Z. Liu, Y. Yang, L. Zhang, P. Sun, Z. Liu, J. Lu, H. Xiong, Y. Peng, S. Tang, Study on the performance of ramie fiber modified with ethylenediamine, *Carbohydr. Polym.* 71 (2008) 18–25.
 [21] C. Yin, J. Li, Q. Xu, Q. Peng, Y. Liu, X. Shen, Chemical modification of cotton cellulose in supercritical carbon dioxide: synthesis and characterization of cellulose carbamate, *Carbohydr. Polym.* 67 (2007) 147–154.
 [22] T. Budinova, N. Petrov, J. Parra, V. Baloutzov, Use of an activated carbon from antibiotic waste for the removal of Hg(II) from aqueous solution, *J. Environ. Manage.* 88 (2008) 165–172.
 [23] R.K. Gupta, R.A. Singh, S.S. Dubey, Removal of mercury ions from aqueous solutions by composite of polyaniline with polystyrene, *Sep. Purif. Technol.* 38 (2004) 225–232.
 [24] M.V. Balarama Krishna, D. Karunasagar, S.V. Rao, J. Arunachalam, Preconcentration and speciation of inorganic and methyl mercury in waters using polyaniline and gold trap-CVAAS, *Talanta* 68 (2005) 329–335.
 [25] F. Zhang, J.O. Nriagu, H. Itoh, Mercury removal from water using activated carbons derived from organic sewage sludge, *Water Res.* 39 (2005) 389–395.
 [26] T.S. Anirudhan, L. Divya, M. Ramachandran, Mercury(II) removal from aqueous solutions and wastewaters using a novel cation exchanger derived from coconut coir pith and its recovery, *J. Hazard. Mater.* 157 (2008) 620–627.